Mineralogy and Petrology (2006) 88: 47–68
DOI 10.1007/s00710-006-0146-4

Mineralogy and Petrology
Printed in Austria

Coexisting calderite and spessartine garnets in eclogite-facies metacherts of the Western Alps

B. Cenki-Tok* and **C. Chopin**

Laboratoire de Géologie, UMR 8538 du CNRS, Ecole normale supérieure, Paris, France
* Present address: Centre de Géochimie de la Surface – EOST, 1 rue Blessig, 67083 Strasbourg Cedex, France (Benedicte.Cenki-Tok@illite.u-strasbg.fr)

Received October 5, 2005; accepted March 8, 2006
Published online August 22, 2006;
Editorial handling: A. Mogessie

Summary

The coexistence of a colourless and a yellow garnet was observed in eclogite-facies manganese concentrations of the Mesozoic ophiolitic Zermatt-Saas Unit, at the Praborna mine near Saint-Marcel, Val d'Aoste, Italy, and in the upper Maurienne Valley, France. They occur both in oxidised metachert with hematite and braunite (+ minor Mn-pyroxenoid and tirodite, rare tiragalloite; with ardennite or piemontite in distinct layers), and in more reduced, carbonate-rich boudins included in it. The co-occurrence takes a variety of textural aspects, from coexisting euhedral garnets (10–100 μm in size for the calderite to mm-size for spessartine) to sharp overgrowths of yellow calderitic garnet on colourless spessartine, to yellow cauliflower-like masses (a few hundreds of μm in size) overgrowing colourless spessartine and showing evidence of oscillatory zoning, resorption stages and resumed growth. Sector zoning and anisotropy are common, although not consistent features.

Compositions can be expressed to 95% in the quadrilateral system (Ca, Mn^{2+})$_3$ (Al, Fe^{3+})$_2$ Si_3O_{12}, with less than 1.0 wt% MgO and 0.8 wt% TiO_2 in colourless spessartine, and less than 0.2 wt% MgO and 1.6 wt% TiO_2 in yellow garnet. Calcium partitions into the ferric garnet. Coexisting pairs define two compositional gaps, bounded by values of the $Fe^{3+}/(Al + Fe^{3+})$ ratio of 10 and 15% for the first one, of 40 and 65% for the other. The optically obvious discontinuity (colour change and Becke's line) corresponds to the narrower gap, between colourless spessartine and yellow spessartine, whereas the broad compositional gap occurs within yellow garnet, between yellow spessartine and yellow calderite, and is only revealed by back-scattered electron images. Only the latter can be a candidate for a miscibility gap, if any.

Introduction

Calderite, $Mn_3Fe^{3+}{}_2Si_3O_{12}$, is the manganese ferric end-member silicate garnet. Calderitic garnet, greenish-yellow under the optical microscope, is relatively rare

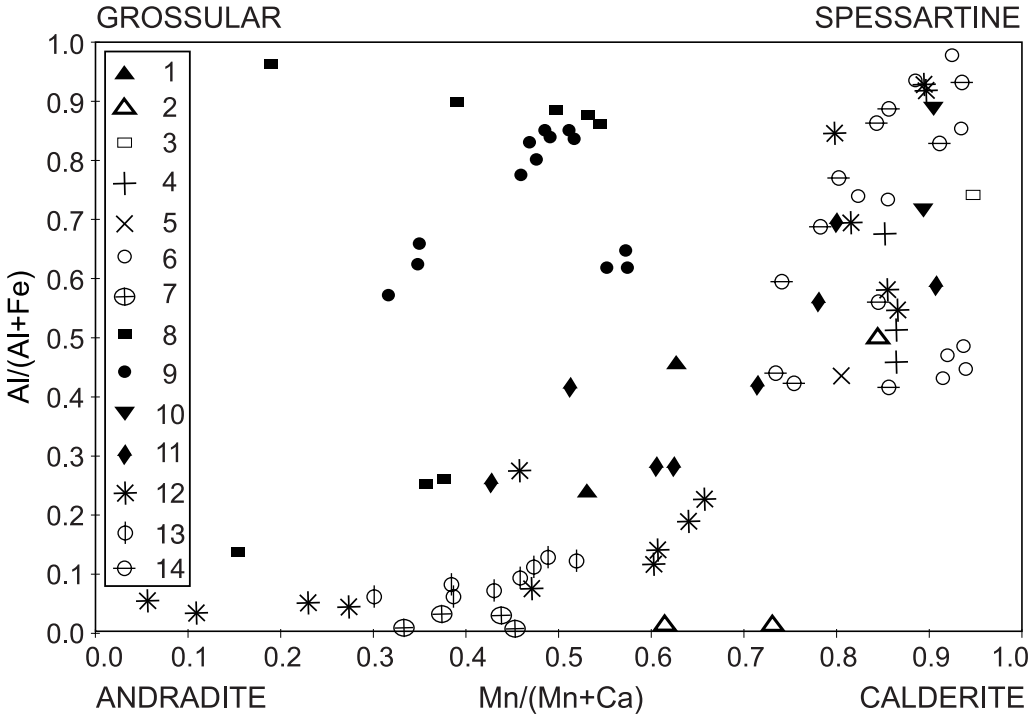

Fig. 1. Occurrence and composition of calderitic garnet: literature data projected in the Ca–Mn–Al–Fe^{3+} quadrilateral. 1: Amphibolite-facies, Namibia (*Vermaas*, 1952; *Dunn*, 1979). 2: Amphibolite facies (0.6–1.0 GPa, 600–650 °C), Labrador, Canada (*Klein*, 1966); with rhodonite, kutnahorite or rhodochrosite, and hematite. 3: Amphibolite-facies, Maharastra, India (*Sastri*, 1963). 4: External zone of a contact aureole (P = 1.0–1.2 GPa), Brezovica, Serbia (*Schreyer* and *Abraham*, 1977), with howeite, amphibole, apatite and ferristilpnomelane. 5: Blueschist facies, Laytonville, California (*Muir Wood*, 1982); with rhodonite, grunerite, kutnahorite and deerite. 6: Amphibolite-facies (0.6 GPa, 600–650 °C), Maharastra, India (*Dasgupta* et al., 1987); with braunite, pyroxmangite, rhodochrosite, jacobsite, quartz and hematite. 7: Blueschist facies (>1.0 GPa, 450–500 °C), Andros, Greece (*Reinecke*, 1987); with quartz, rhodonite, rhodochrosite, deerite, magnetite, barite, androsite-(La). 8: Orthogneiss (UHP or 0.5 GPa? 400–500 °C), Su–Lu, eastern China (*Enami* et al., 1995); overgrowth on grossular-almandine garnet in gneiss with quartz, microcline, albite, biotite, epidote, hematite, titanite and zircon). 9: Ultrahigh-temperature granulite facies, Eastern Ghats, India (*Mukhopadhyay* et al., 2002); with tephroite, clinopyroxene, hausmannite, apatite, Mn-rich calcite, ±bustamite, magnetite. 10. Eclogite facies, Praborna, W. Alps (*Martin* and *Kiénast*, 1987); with hematite, Mn-pyroxenoid, tirodite and quartz. 11. Amphibolite facies, Gamsberg, Namaqualand, S. Africa (*Stalder* and *Rozendaal*, 2005); with rhodonite, hematite or magnetite, calcite, Mn–Zn-spinel, quartz. 12. Amphibolite facies, Otjosondu, Namibia (*Bühn* et al., 1995), with braunite, jacobsite, rhodonite, etc. 13. Same locality as 12 (*Amthauer* et al., 1989). 14. Greenschist facies? Delinesti, Romania, with spessartine, aegirine, pyrophanite, hematite, etc (wet-chemical analyses, *Hàrtopanu* et al., 1997)

in nature (caption to Fig. 1), although favourable rock-compositions are common. It occurs in Mn-rich metasediments, in which the aluminous counterpart spessartine, $Mn_3Al_2Si_3O_{12}$, is normally very common. Calderite and spessartine may indeed occur in neighbouring rocks (e.g. *Bühn* et al., 1995); however, their coexistence has been reported only once (calderite in cross-cutting veins or as overgrowth on earlier spessartine, Fig. 6 in plate II of *Hârtopanu* et al., 1997). In this contribution, we report their coexistence in Mn-deposits metamorphosed under blueschist- to eclogite-facies conditions in the Western Alps. This coexistence raises two problems. The first one deals with the nature of the solid solution between aluminous and ferric Mn-garnets, in particular whether a miscibility gap exists along this join. This is a long-standing problem in the calcic system between grossular, $Ca_3Al_2Si_3O_{12}$, and andradite, $Ca_3Fe^{3+}{}_2Si_3O_{12}$. In oscillatory zoned hydrothermal garnet formed at 300–400 °C, *Jamtveit* (1991) observed two compositional gaps, one for molar fractions of andradite (X_{And}) between 0.20 and 0.35, the other one between X_{And} 0.65 and 0.90. He interpreted the latter as a miscibility gap because of the agreement with the gap predicted at these temperatures by the subregular solution model of *Engi* and *Wersin* (1987) for this system, based on the experimental work of *Huckenholz* and *Fehr* (1982). However, direct textural evidence for immiscibility, like exsolution, has not been reported yet.

The second problem is that the compositional range observed is also controlled by the thermodynamic stability of calderite, which is much more restricted than that of andradite. Indeed, experimental studies suggest that calderite is a high-pressure phase (*Lattard* and *Schreyer*, 1983), with a stability field limited on the high-temperature and low-pressure side by the reaction

$$\text{calderite} = Fe_2O_3\ (\text{hematite}) + MnSiO_3\ (\text{pyroxmangite}) \qquad [1],$$

running at about 2 GPa at 700 °C and 3 GPa at 850 °C.

The products of this simple reaction as well as equivalent assemblages such as pyroxenoid–spinel are quite common in metamorphosed Mn-ores, suggesting that uncommon conditions are required for calderite formation, like high pressure (P) or low temperature (T). Oxygen fugacity (fO_2) also plays a role since, at least in the experiments, calderite only appears in a narrow fO_2 range around the hematite/magnetite buffer (*Lattard* and *Schreyer*, 1983). However, the occurrence in nature of calderitic garnets over a range of P–T conditions, from the blueschist to the granulite facies (Fig. 1), points to the possible stabilising effect of additional components.

On the basis of a petrographic study of two occurrences of associated calderite and spessartine, we aim at (i) constraining the nature of the calderite–spessartine solid-solution, which is controlled by Al–Fe^{3+} substitution in the octahedral site, (ii) accounting for the origin of the observed textures and assemblages in the light of intensive and extensive parameter variations.

Geological setting

The Mesozoic sedimentary sequence associated with the ophiolites of the Western Alps, i.e. the ''Schistes lustrés'' formation, hosts a number of manganese concentrations in radiolarites or siliceous strata. These sediments belong to the lower part

of the section deposited on the Jurassic, Tethyan ocean floor, either on pillow lavas or hydrothermally altered metabasites, or directly on gabbro or serpentinite. This sequence was metamorphosed during Alpine subduction and collision, from lowest-grade blueschist-facies conditions in the external units (e.g. *Martin* and *Polino*, 1984; *Martin* and *Lombardo*, 1995) to eclogite-facies conditions in the internal units (*Gruppo Ofioliti*, 1977), locally reaching coesite-eclogite conditions (*Reinecke*, 1991). The two localities studied belong to the eclogite-facies Zermatt-Saas Unit (e.g. *Dal Piaz* et al., 2001), which structurally overlies the Monte Rosa and Gran Paradiso internal crystalline massifs. The Ouille du Midi locality belongs to a small group of concentrations occurring at the upper end of the Maurienne Valley, France (*Chopin*, 1978), on the western tip of the Gran Paradiso massif. The Saint-Marcel locality is the famous Praborna mine, in Val d'Aosta, Italy, on the north-eastern flank of the Gran Paradiso massif and immediately overlain by the Austro-alpine Mt Emilius klippe (*Martin* and *Kiénast*, 1987). In either locality the presence of eclogitic metabasite (with paragonite and glaucophane stable) and of the talc–chloritoid–garnet ($\pm$ phengite) assemblage in metapelite (*Chopin*, 1981a, b) [the latter magnificently developed near Praborna, at the Servette mine (*Martin* and *Tartarotti*, 1989)] points to peak conditions on the order of 1.5 GPa, 500 °C. These may be marginally lower in Maurienne (1.25 ± 0.3 GPa, 480 ± 50 °C, *Rolland* et al., 2000) as compared to Val d'Aosta ($P > 1.0$–1.2 GPa, 500–600 °C; *Martin* and *Tartarotti*, 1989; *Dal Piaz* et al., 2001).

Occurrence and mineralogy

In Maurienne, a few small Mn deposits occur as quartz-rich lenses intercalated within several-metre-thick, mappable layers of quartz–phengite–almandine schist ('Radiolarites' on the 1:50,000 geological map, *Fudral* et al., 1994) in a series of calcschist and metashale overlying bodies of serpentinite with ophicalcite and minor metabasite. The lenses show a strong compositional layering among the main phases quartz, braunite, hematite, spessartine, ardennite and piemontite. These 'oxidised assemblages' imply several oxidation states of manganese and essentially trivalent iron. In some lenses, a black weathering crust signals decimetre-size quartz-poor to quartz-free pods that consist of either rhodochrosite and Mn-silicates (pyroxmangite, tephroite, friedelite, Mn humites), or of Mn-silicates (tephroite, humites, chlorite) and spinels (galaxite, jacobsite). In both cases the assemblages contain only divalent Mn, i.e. are 'reduced'. These mineralogical and chemical variations across the lenses most likely reflect the original compositional banding of the protolith. For more details the reader is referred to *Chopin* (1978) for the mineral assemblages, to *Pasero* and *Reinecke* (1991) and *Pasero* et al. (1994) for ardennite. Since then, in one such lens on the slopes of Ouille du Midi (OM), we found calderitic garnets in two rock-types: oxidised braunite-quartzite showing the strong compositional layering mentioned above (sample series OM-Mn and Ard) and a small massive, pink to grey Mn-silicate–carbonate pod (OM-96M).

The Praborna mine in Saint-Marcel (SM) is a classical locality from which a number of Mn minerals have been described, like piemontite (*Kenngott*, 1853), roméite (*Damour*, 1841; *Brugger* et al., 1997) and strontiomelane (*Meisser* et al.,

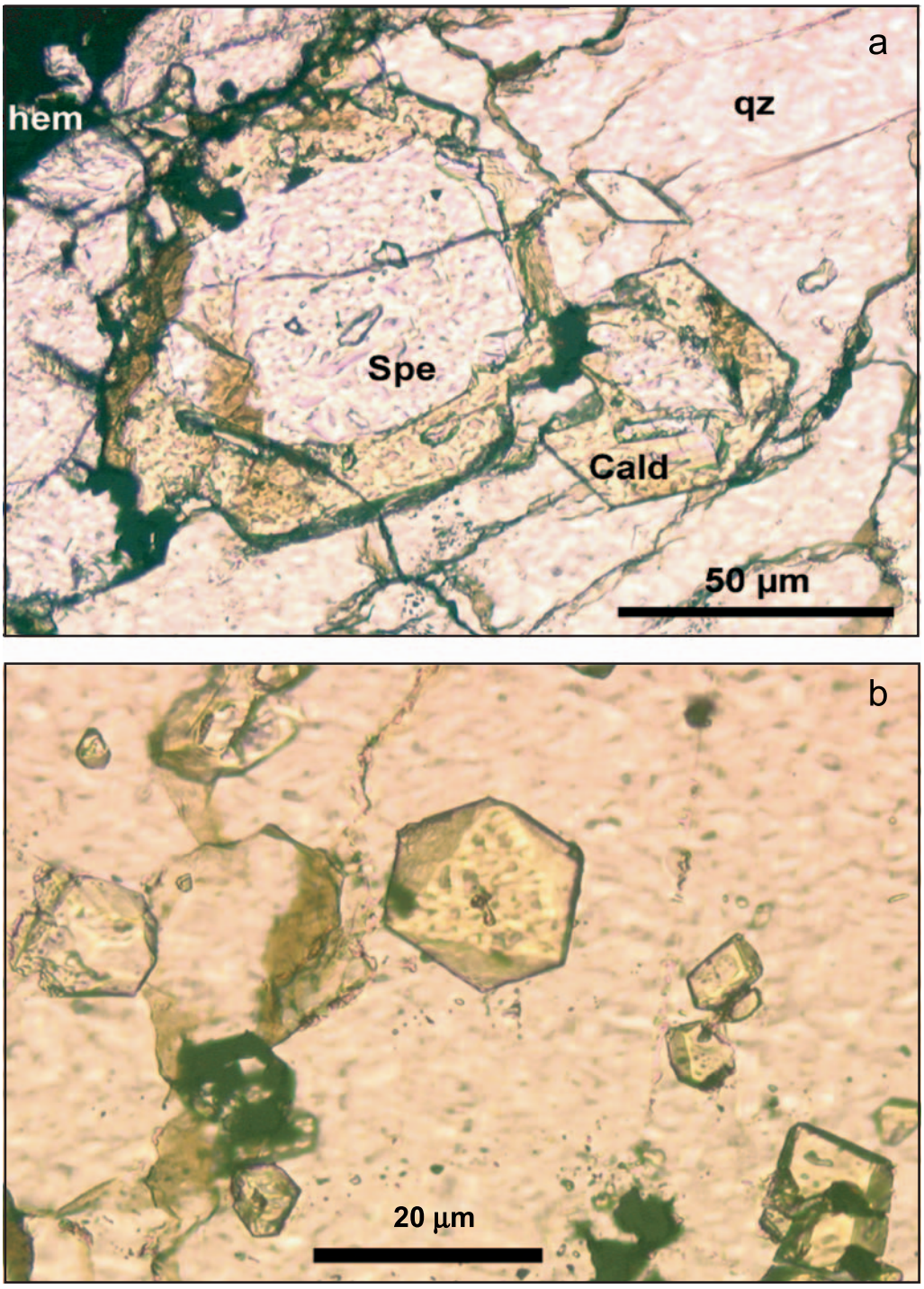

Fig. 2. **a** Typical overgrowth of yellow garnet on colourless spessartine. Note the Becke line between core and overgrowth. **b** Octahedral yellow garnet in quartz. Both: photomicrographs, plane polarised light, quartzite sample # Ard, Ouille du Midi

1999), not to mention the spectacular colour varieties of pyroxene, phengite, titanite, etc (e.g. *Bondi* et al., 1978; *Brown* et al., 1978; *Mottana* et al., 1979). A fine geological and petrological description is given by *Martin* and *Kiénast* (1987) and *Tumiati* (2005), to which the reader is referred for details. The situation and structure of the deposit, with a layered oxidised quartzite horizon containing the braunite ore but also some reduced boudins of Mn carbonate–silicates assemblages, are basically the same as in other deposits of the Val d'Aosta or the Maurienne valley, yet with a greater thickness and areal extension. We found calderite in two composite samples collected on the mine dumps, macroscopically described below. One [SM54] shows the contact between a pink pyroxenoid–rhodochrosite fels and spessartine quartzite, in a single thin section. The other [SM56], is a two-fist-size block of vein quartz containing abundant brecciated fragments of a dismembered yellow, very spessartine-rich bed and a larger, about 5 cm cockade. The dark greyish-brown cockade core consists of fine-grained tephroite (partly serpentinised) and rhodochrosite (thin section SM56-5, with calderite, hematite and minor pyrophanite, jacobsite and manganiandrosite-(Ce) [vote 2002-49 of the IMA-CNMMN, *Cenki-Tok* et al., 2006; cf. *Bonazzi* et al., 1996]). This core is surrounded by a centimetre-thick pink spary reaction rind of rhodochrosite and Mn-pyroxenoid (along with scattered crystals of spessartine, calderite, hematite and pyrophanite, section SM56-2) passing, through increasing modal amounts of spessartine, to a yellowish outer rim. The cockade represents a fragment of a carbonate-rich, Si-undersaturated protolith and its successive reaction zones with the vein quartz (a more complete description is in *Cenki-Tok* et al., 2006). To our knowledge calderite is new to Praborna; the closest and sole approach was a zoned spessartine crystal analysed by *Martin* and *Kiénast* (1987) in hematite–Mn-pyroxenoid quartzite, showing a ferrian rim on a nearly Fe-free core (no. 10 in Fig. 1).

Some samples devoid of calderitic garnet may give hints as to bulk-chemical controls on the appearance of this garnet. For instance, the silica-deficient but Al-rich, Mn-chlorite–galaxite–jacobsite assemblage in Le Villaron Mn-ore body, near Ouille du Midi, does not bear calderite (*Chopin*, 1978). Similarly, in the quartz–braunite ore at Ouille du Midi, calderitic garnet is typically absent from the layers containing other Mn–Al-silicates in addition to spessartine, like piemontite and ardennite. Clearly the more alumina-rich compositions of these systems prevented calderite occurrence. In Saint-Marcel, green pods in quartzite (SM-57) consist of clinopyroxene, spessartine, epidote, titanite, hematite; these less Mn-rich and, again, more Al-rich bulk compositions were not suitable for calderite formation.

Petrography, textural relationships of garnets

In hand specimen calderite crystals cannot be distinguished from the millimetre-sized spessartine crystals. In transmitted light two garnet phases are conspicuous: colourless spessartine and a greenish to yellow garnet, referred to as calderitic. This practical colour distinction is retained for the micro-petrographic description, even if calderitic garnet, i.e. yellow garnet, will be shown later to be either Al-dominant (then referred to as yellow or calderitic spessartine), or Fe^{3+}-dominant (then referred to as calderite). Given the composite or layered nature of most samples, the petrographic description is more conveniently made according to a

few generic rock types that may occur side by side in a given sample. These are quartz–braunite ore, spessartine quartzite and pyroxenoid–rhodochrosite fels.

Quartz–braunite ore (sample OM-Mn) is the most oxidised rock type, with trivalent Mn expressed in braunite and piemontite. Locally lensoid aggregates containing macroscopically yellow garnet (mostly spessartine) appear within the gneissosity. Attesting to an early assemblage, small (20–100 μm) crystals of apatite, braunite, rutile, piemontite and rare pyrophanite are preserved as inclusions in some colourless garnets. The main rock-forming assemblage, with some compositional layering, includes poikilitic, colourless garnet, quartz, braunite, carbonate, Mn-pyroxenoid, tiragalloite ($Mn_4AsSi_3O_{12}(OH)$, a new occurrence, cf. *Gramaccioli* et al., 1980) and yellow garnet, although there is locally evidence that the latter postdates the main assemblage. Retrograde manganocummingtonite and carbonate developed locally, and coatings of Mn higher oxides are supergene. This is the sole rock type in which calderitic garnet reaches a relatively large size (50–200 μm); it is pale yellow, zoned, with anisotropic extinction and sector-twinning. Locally yellow garnet forms blurred isotropic overgrowth (<30 μm) on poikilitic, colourless spessartine crystals (100–300 μm). Quartz grains commonly mark the boundary between the two garnet phases. Rarely small yellow calderite crystals (<30 μm) grow at the grain boundaries of coexisting colourless spessartine, pyroxenoid, hematite and braunite crystals. Ardennite and piemontite coexist in other layers.

Spessartine quartzite (SM54 *pro parte*, SM56 *pp*, OM-Mn *pp*, Ard) is a less oxidised rock type, bearing mostly divalent Mn but essentially trivalent Fe. Large (up to mm-size) colourless spessartine crystals contain quartz and opaque inclusions, and, together with quartz, rhodochrosite, hematite, pyrophanite and pyroxenoid, make most of the mineral assemblage. In addition, coarse yellow manganoan aegirinic diopside and amphibole occur locally in sample SM56. Yellow garnet (Fig. 2) forms systematic over- and inter-growths (<100 μm) around and along poikilitic, colourless spessartine crystals (200–600 μm) shielded in the quartz matrix. The contact is blurred or sharp; in the latter case it can be crystallographically controlled (Fig. 3a). Locally yellow calderite also appears as tiny single crystals (<100 μm) included in late developed quartz areas, or forms thin amoebic arms interstitial to matrix quartz.

The rhodochrosite–Mn-pyroxenoid fels (SM54 *pp*, SM56 *pp*, OM-96M) occurs as pods or layers within spessartine quartzite. It is a relatively reduced (divalent Mn and mostly trivalent Fe) and carbonate-rich, silica- and alumina-poor rock type. Quartz-free parts bear tephroite in both localities (SM56-5, OM-96M). Pyrophanite is a common accessory, along with manganiandrosite-(Ce) in SM54 and SM56, and with rare titanite in OM-96M; all are anhedral and fine-grained. Yellow garnet is absent from the pink fels part of SM54 but occurs in the other samples as heaps of small euhedral isotropic crystals (10–50 μm) arranged in necklace texture in the carbonate groundmass, and as overgrowth (<100 μm) on and along fractures in a few scattered poikilitic, colourless spessartine crystals (100–300 μm).

Backscattered-electron (BSE) images reveal that, in quartz–braunite ore and spessartine quartzite, three rather than two garnet phases can be distinguished (Fig. 3b–d). The darker phase in BSE is richer in Al and corresponds to the colourless spessartine. The brighter and the intermediate phase are richer in Fe, both appear yellow in transmitted light and they correspond to yellow calderite and yellow

Table 1. *Representative EMP analyses of coexisting Mn-rich garnets in the main rock-types*

wt%	Spessartine quartzite, SM 54			Rhodochr.-pyroxenoid fels, OM 96			Quartz–braunite ore, OM Mn1		
	spessartine core	calderite rim	interm. garnet transition	spessartine euhedral	calderite euhedral	spessartine core	interm. garnet rim	interm. garnet euhedral	spessartine low Ti
SiO_2	35.92	34.13	35.46	36.98	33.54	36.92	35.06	36.11	36.90
TiO_2	0.77	0.84	0.42	0.07	0.45	0.19	1.58	0.31	0.12
Al_2O_3	19.26	4.56	14.95	20.11	1.74	19.41	11.69	15.73	20.17
Fe_2O_3	2.09	22.14	7.40	0.09	26.02	2.30	11.47	6.51	1.55
MnO	34.55	25.35	37.09	38.70	26.47	34.41	31.71	37.28	36.27
MgO	0.55	0.14	0.13	0.21	0.12	0.70	0.07	0.12	1.01
CaO	7.08	12.70	4.30	3.57	11.60	5.83	8.25	3.30	4.87
Na_2O	0.03	0.03	0.07	0.00	0.04	0.03	0.07	0.00	0.00
	100.24	99.88	99.82	99.74	99.98	99.79	99.90	99.36	100.89
Basis: 5 non-tetrahedral cations									
Si	2.87	2.94	2.96	3.04	2.94	3.01	2.94	3.06	2.95
Ti	0.05	0.05	0.03	0.00	0.03	0.01	0.10	0.02	0.01
Al	1.81	0.46	1.47	1.95	0.18	1.87	1.16	1.57	1.90
Fe tot	0.13	1.44	0.46	0.01	1.72	0.14	0.73	0.42	0.09
Mn tot	2.34	1.85	2.62	2.70	1.96	2.38	2.26	2.68	2.46
Mg	0.07	0.02	0.02	0.03	0.02	0.08	0.01	0.02	0.12
Ca	0.61	1.17	0.38	0.32	1.09	0.51	0.74	0.30	0.42
Na	0.00	0.00	0.01	0.00	0.01	0.00	0.01	0.00	0.00
$Al/(Al+Fe)$	0.94	0.24	0.76	1.00	0.09	0.93	0.61	0.79	0.95
$Mn/(Mn+Ca)$	0.79	0.61	0.87	0.90	0.64	0.82	0.75	0.90	0.85

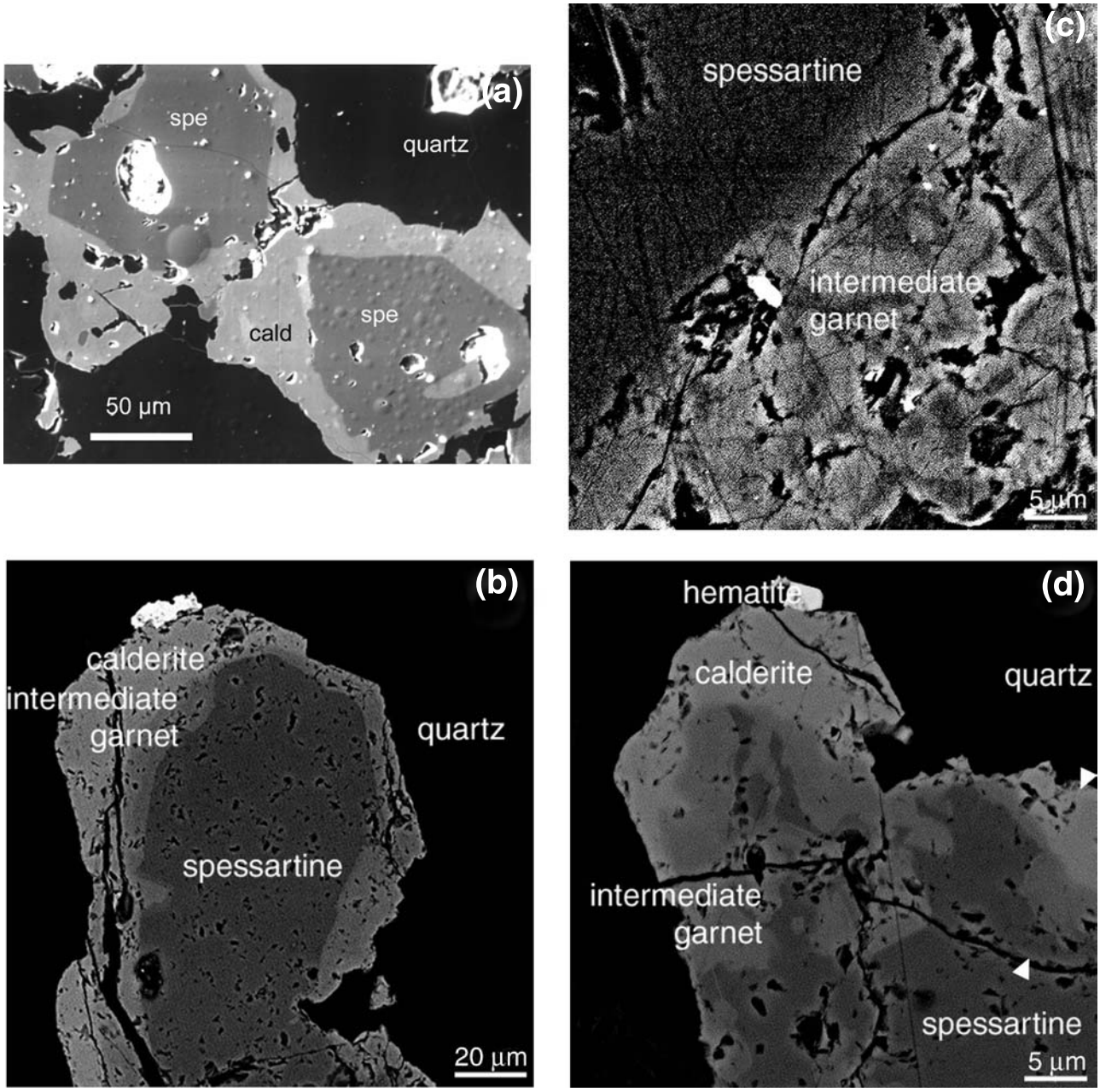

Fig. 3. BSE images of calderitic overgrowths (light) on spessartine cores (dark). **a** Simple overgrowth, with no evidence of resorption at the interface (#Ard 2a; the bright spots are artifacts). **b** Complex overgrowth. Note the embayment (resorption of the core), the growth of an intermediate zone, then of the outer calderite rim (#SM-54). **c** Cauliflower-like overgrowths of yellow garnet on colourless spessartine, with evidence of oscillatory zoning (right hand side of the picture; #OM-Mn). **d** Calderite envelope on spessartine-intermediate garnet intergrowth (#SM-54). Note the highly corroded remnants of high-Al spessartine within the intermediate zone (upper left quarter), whereas the contact between intermediate and outer zone is smoother (along rational planes?), as in (b). The arrowheads on the right-hand side indicate the profile shown in Fig. 6

spessartine, respectively. At the Ouille du Midi locality, brighter and intermediate garnet form complex intergrowths (Fig. 3c) in spessartine quartzite and quartz–braunite ore. The large euhedral anisotropic yellow garnet crystals in the latter rock type are also of intermediate composition, whereas, both in the carbonate rock and the quartzite, the strings of small yellow calderite (Fig. 2b) are extremely rich in Fe^{3+} and can also directly overgrow the colourless spessartine (Figs. 2a, 3a). In the Saint-Marcel quartzite samples, the three garnet phases are well represented. The darker and brighter garnets [colourless spessartine and yellow calderite] are commonly not in contact but are separated by a rim of intermediate garnet [yellow spessartine] (Fig. 3b–d), with the sequence: darker garnet core, darker and intermediate garnet intergrowths, brighter garnet rim sharply overgrowing the envelope of the intergrowths.

In summary, whatever the locality and the rock-type, the growth of a yellow calderitic garnet postdates that of colourless spessartine. This yellow garnet is only of intermediate, spessartine composition in quartz-braunite ore (OM), only of calderite composition in the carbonate–pyroxenoid fels (OM and SM), and grades from intermediate spessartine to calderite in the quartzites (SM mostly, OM).

Chemistry of coexisting garnets

Analytical procedure

Electron-microprobe (EMP) analyses were performed with a Cameca Camebax apparatus at University Paris 6 (15 kV, 15 nA, 10–30 s counting time on peak, and natural and synthetic standards: diopside (Si, Mg, Ca), anorthite (Al), albite (Na), orthoclase (K), Fe_2O_3, $MnTiO_3$ (Mn, Ti), AsGa (As). Garnet formulae are recalculated on a fixed number of cations, which makes the result independent of the actual valence state of Fe and Mn. Considering the possibility of a hydrogarnet component, all cations are calculated on the basis of 5 non-tetrahedral cations, a procedure that admittedly amplifies any analytical error on the major cation Si [for which an andradite standard could have been more appropriate (D. Lattard, pers. comm.)] and ignores tetrahedral ferric iron. Silicon and arsenic if any are assigned to the tetrahedral site. The octahedral site is first filled with aluminium, titanium and iron. If their sum is larger than 2, the remaining Fe is assigned to the dodecahedral site and can form a 'skiagite' ($Fe^{2+}{}_3Fe^{3+}{}_2Si_3O_{12}$) component. If the sum is lower than 2, the octahedral deficit is filled by Mn which may form a 'blythite' ($Mn^{2+}{}_3Mn^{3+}{}_2Si_3O_{12}$) component.

Results and a graphical representation

The average atomic Si content per formula unit (pfu) obtained for colourless garnet as well as for yellow garnet is 2.97, implying a negligible hydrogarnet component, if any. This is confirmed by analytical totals close to 100 wt% if all Fe is considered trivalent, as indicated by the structural formulae. Accordingly, the $^{[4]}$Al (or $^{[4]}$Fe) percentage is always low and was ignored in the following. Likewise the 'blythite' or 'skiagite' percentage calculated for most garnets is lower than 1.1 mol%, except for a few analyses of yellow garnet in sample OM-Mn1 that show 'blythite' con-

Table 2. *Representative EMP analyses of coexisting carbonate (carb) and Mn-pyroxenoid (pxd) in the main rock-types, and of tiragalloite*

wt%*	Quartzite SM 54		Rhodochr.-pyroxenoid fels OM 96				Qtz-braunite ore OM Mn1		
	pxd	carb	pxd a	pxd b	carb a	carb b	pxd	carb	tiragal.
SiO_2	45.90		46.40	46.43			46.69		31.20
As_2O_5									16.06
V_2O_5									0.85
FeO tot	0.35	0.16	0.43	0.24	0.09	0.11	0.00	0.12	0.17
MnO	51.34	55.45	51.48	48.50	55.95	53.59	51.18	49.78	47.70
MgO	0.49	0.43	1.30	2.24	0.99	2.06	1.18	2.29	0.21
CaO	1.36	3.19	1.28	2.36	2.84	4.15	2.03	6.05	0.63
Total	99.42	59.24	100.88	99.76	59.88	59.91	101.08	58.24	96.81
Cation basis	2	1	2	2	1	1	2	1	8
Si	0.999		0.991	0.992			0.994		3.06
As									0.82
V									0.06
Fe	0.006	0.003	0.008	0.004	0.001	0.002	0.000	0.002	0.01
Mn	0.947	0.918	0.931	0.878	0.912	0.856	0.923	0.808	3.96
Mg	0.016	0.012	0.041	0.071	0.028	0.058	0.037	0.065	0.03
Ca	0.032	0.067	0.029	0.054	0.059	0.084	0.046	0.124	0.07

* Na_2O, Al_2O_3 and TiO_2 all <0.05 wt%

tents up to 9.8 mol% (for a negligible $^{[4]}$Al component). Magnesium is consistently low and partitioned into colourless garnet (<1 wt% MgO in colourless garnet; <0.2 wt% MgO in yellow garnet; Table 1). Titanium is a minor component preferentially incorporated into yellow garnet (<0.8% vs. <1.6% TiO_2 in colourless and yellow garnet, respectively; Table 1). Other elements like Na, V, As or P are below or close to EMP detection limit, even in the presence of tiragalloite (analysis in Table 2, along with those of coexisting carbonate and Mn-pyroxenoid). Therefore, the chemistry and compositional variations of the studied garnets are accounted for to more than 95 mol% by the four components $Ca_3Al_2Si_3O_{12}$, $Mn_3Al_2Si_3O_{12}$, $Ca_3Fe^{3+}{}_2Si_3O_{12}$ and $Mn_3Fe^{3+}{}_2Si_3O_{12}$. Hence we chose a quadrilateral chemical representation (Fig. 4) in which the $XFe = Fe/(Fe + Al)$ and $XMn = Mn/(Mn + Ca)$ ratios represent the amount of substitution in octahedral or dodecahedral site, respectively. We definitely recommend the use of this representation, because it avoids the pitfalls of the arbitrary choices inherent to any decomposition of structural formulae into end-member garnets, and to any triangular plot. The $X = 0.5$ lines divide this diagram into the four fields grossular, andradite, calderite and spessartine (Fig. 4c), allowing unique assignment of the proper name to any relevant garnet.

Paragenetic variations

The garnet compositions for each rock type are shown in Fig. 4. In *spessartine quartzite* (Fig. 4a), calderite compositions cluster around $XFe = 0.75$ and $XMn =$

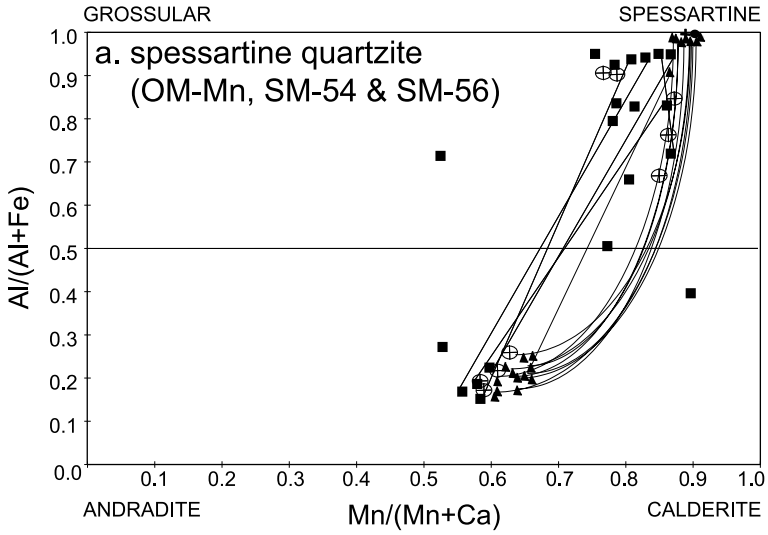
GROSSULAR
SPESSARTINE
a. spessartine quartzite
(OM-Mn, SM-54 & SM-56)
Al/(Al+Fe)
Mn/(Mn+Ca)
ANDRADITE
CALDERITE

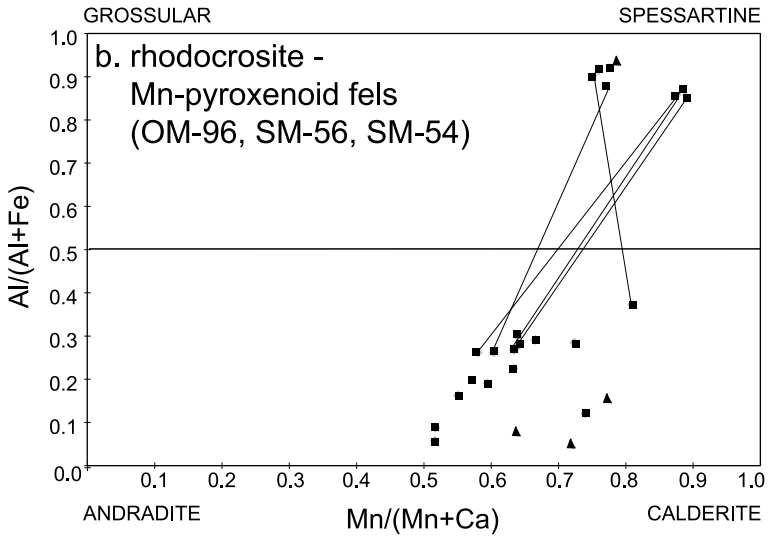
GROSSULAR
SPESSARTINE
b. rhodocrosite -
Mn-pyroxenoid fels
(OM-96, SM-56, SM-54)
Al/(Al+Fe)
Mn/(Mn+Ca)
ANDRADITE
CALDERITE

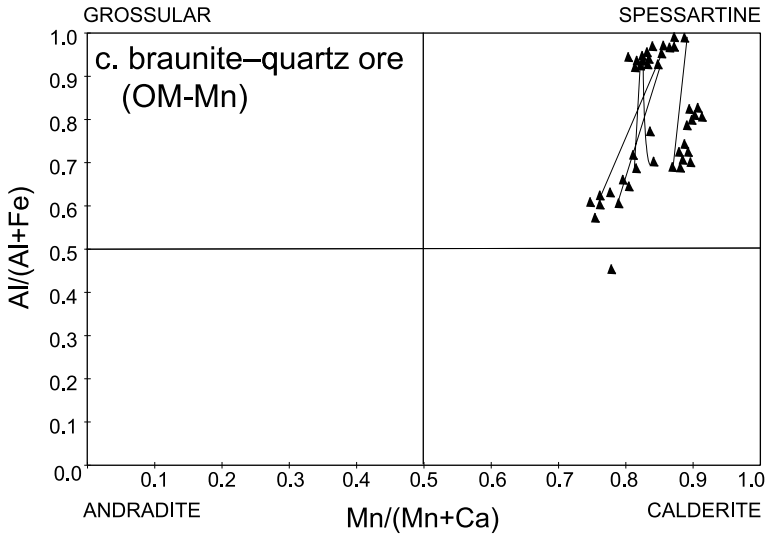
GROSSULAR
SPESSARTINE
c. braunite–quartz ore
(OM-Mn)
Al/(Al+Fe)
Mn/(Mn+Ca)
ANDRADITE
CALDERITE

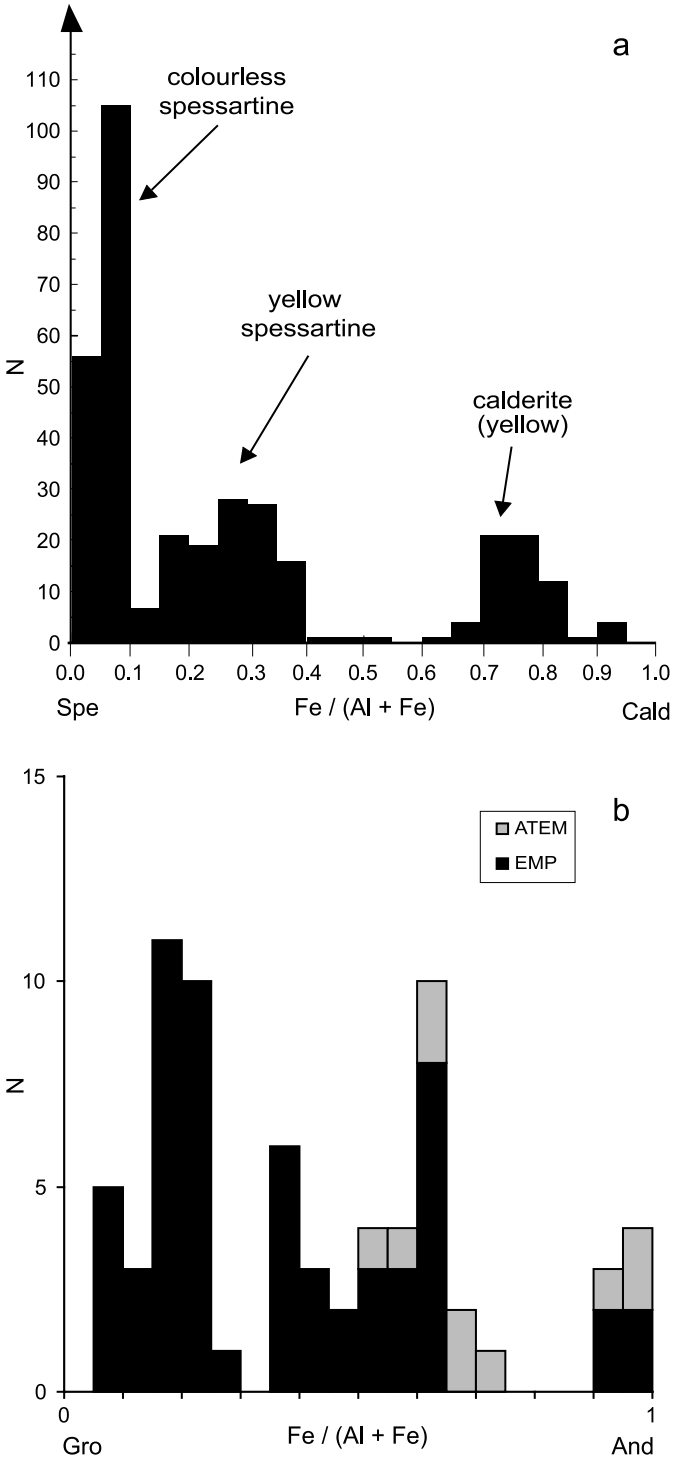

Fig. 5. Histograms showing (**a**) the proportion of octahedral ferric iron in all the garnet analyses of this study (362 EMP analyses); (**b**) the proportion of octahedral ferric iron in grandite garnets studied by *Jamtveit* (1991) and *Pollok* et al. (2001)

Fig. 4. Quadrilateral representation of the chemistry of coexisting garnets ($MgO < 1$ wt%, $TiO_2 < 1.6$ wt%) according to rock types. Squares, Saint-Marcel locality; triangles, Ouille du Midi locality; circled crosses, analyses from profile of Fig. 6. Tie-lines connect compositions of colourless core and yellow rim in a garnet crystal

0.6. These correspond to the sharp yellow garnet overgrowth on both yellow and colourless spessartine, as found in the two localities. For most spessartine garnets XFe ranges between 0.0 and 0.4, the boundary between colourless and yellow colour occurring near XFe = 0.15. Therefore, the common pattern observed is colourless spessartine core, yellow spessartine overgrowth (with or without resorption features) and yellow calderite rim (Fig. 3b, d). Intermediate, 'yellow-spessartine' compositions are widespread in Saint-Marcel but rare at Ouille du Midi in this rock type. In the *rhodochrosite–Mn-pyroxenoid fels* from both localities (Fig. 4b) garnet compositions cluster in two groups, calderite and colourless iron-poor spessartine, without intermediate compositions. Isolated calderite and colourless spessartine crystals show higher iron and aluminium content, respectively, than their counterparts in rare crystals showing overgrowths. In the *braunite–quartz ore* (Fig. 4c; Ouille du Midi only), garnet compositions form two groups. One is close to the spessartine end-member, the other is of intermediate composition (XFe ranges between 0.20 and 0.45) and corresponds to yellow spessartine. In this group, the more Mn-rich analyses pertain to large, euhedral isolated yellow garnet crystals, the less Mn-rich to overgrowths on colourless spessartine. The compositional variations in these overgrowths must be connected to the density contrasts revealed by

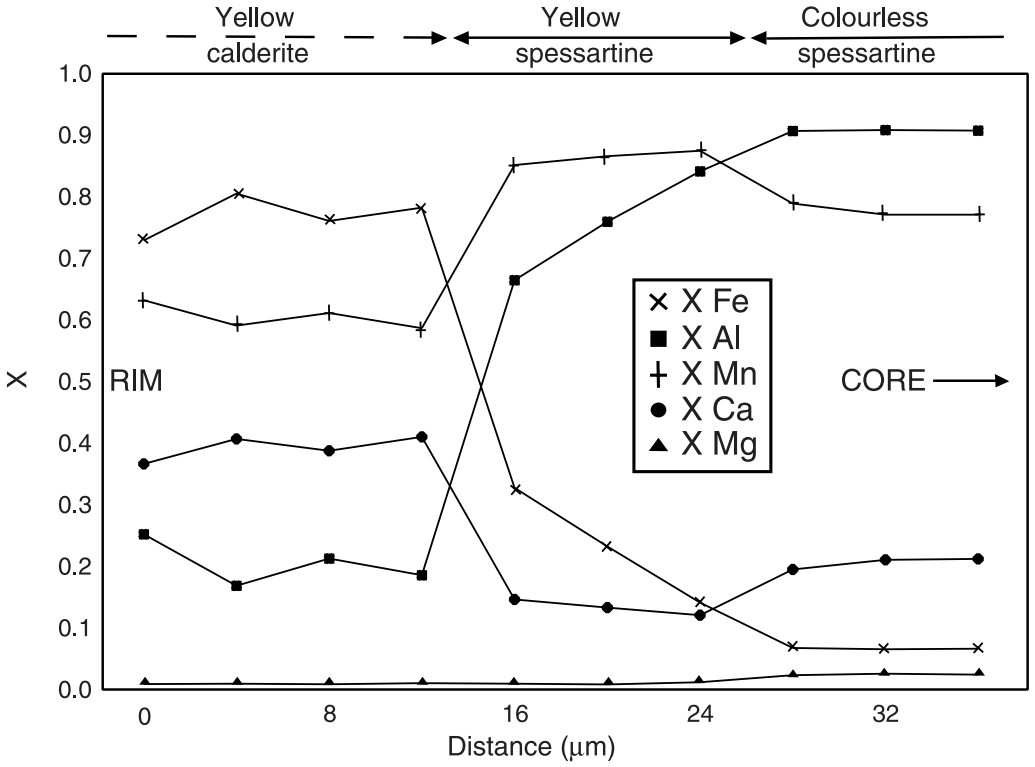

Fig. 6. Analytical traverse (ca. 35 μm) across the contact between spessartine and calderite (#SM-54; see location on Fig. 3d): concentration profiles from EMP analyses. XFe = Fe/(Fe + Al); XAl = Al/(Al + Fe); for this figure XMn = Mn/(Mn + Ca + Mg); XCa = Ca/(Mn + Ca + Mg); XMg = Mg/(Mn + Ca + Mg). Note the Mn and Ca behaviour in the intermediate zone, which precludes the possibility of mixed analyses

BSE pictures (Fig. 3c) that suggest complex, locally oscillatory zoning, below EMP spatial resolution.

Compositional gaps

All the 362 garnet analyses performed are presented with respect to Fe–Al substitution on the histogram of Fig. 5a. This projection highlights the three groups defined above, corresponding to spessartine with XFe = 0.00–0.10 (colourless in thin section, darker zones on BSE images), yellow spessartine with XFe = 0.15–0.40 (yellow in thin section, intermediate brightness in BSE) and calderite with XFe > 0.65 (yellow in thin section, brighter zones on BSE images). Very few analyses (4 out of 362) project in the XFe = 0.40–0.65 range and may represent mixed analyses near zone boundaries. The implied compositional gap is the most obvious candidate for a miscibility gap, if any. Ironically, this large gap defined within yellow-garnet compositions does not match the conspicuous optical discontinuity materialised by the colour change and a Becke's line between yellow and colourless garnet. The latter corresponds to the narrow range XFe = 0.10–0.15, in which only few analyses do project (Fig. 5a).

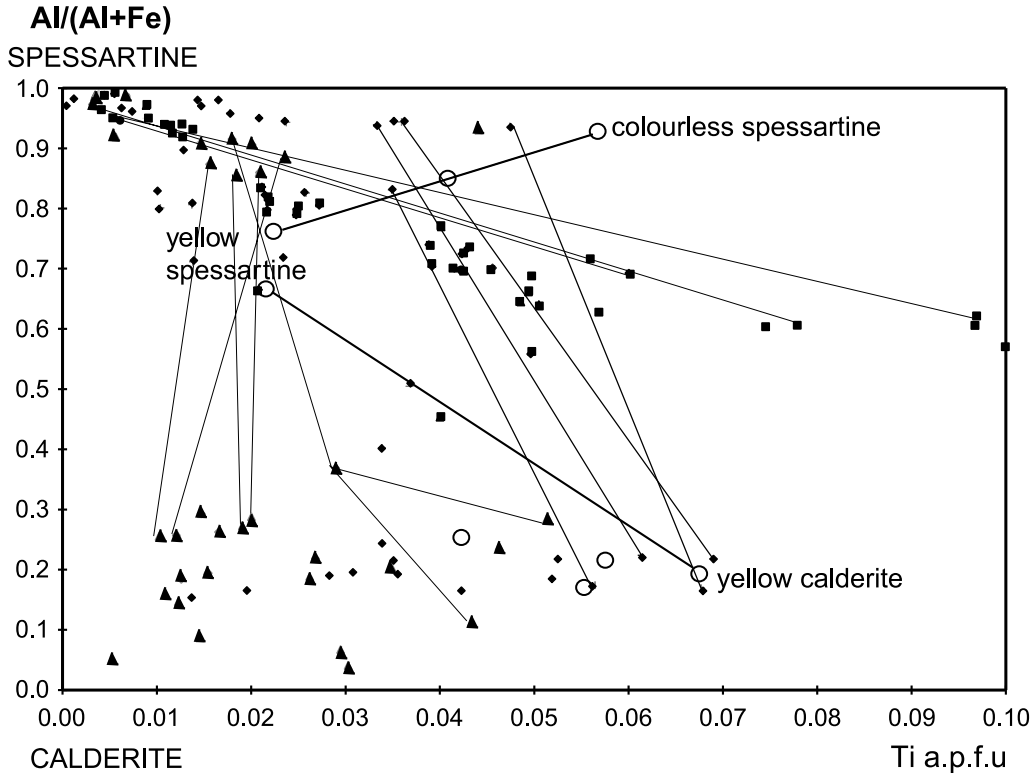

Fig. 7. Titanium content as a function of Al–Fe^{3+} substitution in Mn-rich garnets of Saint-Marcel and Ouille du Midi: in quartz-braunite ore (#OM-Mn1, squares), spessartine quartzite (#SM54, #OM-96M *p.p.*, small diamonds) and rhodochrosite–Mn-pyroxenoid fels (#SM56, #OM-96M, triangles). The larger circles refer to the point analyses of the profile of Fig. 6 and Fig. 3d. The uncertainty on Ti is much larger than symbol size

The nature of these potential gaps was further explored by a compositional profile (Fig. 6; circled crosses in Fig. 4a) across three apparently homogeneous garnet zones (Fig. 3d). Calderite is homogeneous and shows the highest XFe and lowest XMn values (around 0.78 and 0.60, respectively). Colourless spessartine is homogeneous, with the lowest XFe (0.07) and a high XMn value (0.80). Yellow spessartine is not homogeneous, unlike suggested by BSE images. It shows continuously decreasing XFe values (0.32–0.12) which are intermediate between those of calderite and spessartine. In contrast, the XMn value shows only minor variations (around 0.87) but is the highest of all the three zones – which, incidentally, is evidence that none of the three yellow-spessartine analyses can be a linear combination of calderite and colourless spessartine. The two analyses located on either side of the optical and BSE discontinuity give a maximum extent for a compositional gap on the Al-rich side (XFe = 0.08–0.14 and XMn = 0.81–0.89), if any. Yet, the major chemical changes in both dodecahedral and octahedral sites occur at the border between yellow spessartine and calderite: XFe and XMn drastically change from 0.78 to 0.32 and 0.59 to 0.86, respectively.

The minor element Ti provides one more dimension to look at these compositional gaps (Fig. 7). Its partitioning between coexisting colourless and yellow spessartine in quartz–braunite ore shows a quite different pattern from that between directly coexisting colourless spessartine and yellow calderite (in quartzite or carbonate fels), and from that between colourless Ti-rich spessartine and yellow Ti-poor spessartine in quartzite.

Discussion

Crystal chemistry

The analyses of coexisting garnets suggest that Ca and Ti are preferentially incorporated into the calderite-rich crystals. In Fig. 4, the positive slope of the lines linking calderite-rich and calderite-poor clusters shows a coupled incorporation of Fe^{3+} (for Al) and Ca^{2+} (for Mn) into the calderitic garnets, which may reflect a concomitant increase in size of the octahedral and dodecahedral sites. *Jamtveit* et al. (1995) made a similar observation for hydrothermal Mn-poor andradite-rich garnets. In addition, we observe that, in most instances, Ti preferentially enters the ferric garnet (cf. Table 1 and Fig. 7). For andratitic garnets, *Armbruster* et al. (1998) suggested that Ti is incorporated via the schorlomitic mechanism $^{[6]}Ti^{4+} + {}^{[4]}Fe^{3+} = {}^{[6]}Fe^{3+} + {}^{[4]}Si^{4+}$, to which *Chakhmouradian* and *McCammon* (2005) added the $^{[4]}Al$ analogue $^{[6]}Ti^{4+} + {}^{[4]}Al^{3+} = {}^{[6]}Fe^{3+} + {}^{[4]}Si^{4+}$. The small range of Ti contents and the small departure of the Si contents from 3 pfu in our calderite analyses do not allow identification of one particular mechanism.

Another crystallographic particularity of the spessartine–calderite garnets studied here is that they are not always isotropic. This feature is common in grandite garnets (e.g. *Allen* and *Buseck*, 1988) and a variety of possible mechanisms has been proposed to account for the departure from cubic symmetry (reviewed by *Andrut* and *Wildner*, 2001), like partial ordering of Al–Fe in octahedral sites, or of a hydrous component; or strain arising from lattice mismatch at compositional

boundaries in zoned garnets. However, we could not establish any consistent link between anisotropy and composition or paragenesis.

Controls on calderite stability; growth and dissolution features

Experiments as well as other natural occurrences point to the importance of extensive and intensive parameters for the appearance of calderitic garnet. *Lattard* and *Schreyer* (1983) suggested that the formation of end-member calderite is restricted to fO_2 close to the hematite/magnetite buffer. In the grossular–andradite system, *Jamtveit* et al. (1995), considering the different aqueous complexation behaviour of Al^{3+} and Fe^{3+}, showed that Fe^{3+} incorporation in garnet is strongly dependent on temperature, pH, fO_2 and salinity, a higher fO_2 favouring Fe^{3+} incorporation in the solid (garnet). Thus, the composition of the intergranular fluid may play a key role in the appearance of calderitic garnet as well. The deposits studied here were metamorphosed under similar temperature conditions but show quite a range of oxidation states, with layer to layer variations that are inherited from the sedimentary protolith and reflect internal fO_2 buffering by the solids (*Chopin*, 1978, cf. *Bühn* et al., 1995). For the samples bearing calderitic garnet, the relevant fO_2 conditions can be bracketed between 10^{-14}–10^{-7} bar for the spessartine quartzite and rhodochrosite fels (i.e. between the hematite/magnetite buffer and the Mn-pyroxenoid–quartz/braunite buffer), and, for the braunite ore, near 10^{-7} bar with pyroxmangite (e.g. *Abs-Wurmbach* et al., 1983).

The petrographic observations show that the growth of calderitic garnet postdates that of spessartine. Indeed, even if calderitic garnet was able to nucleate independently of pre-existing spessartine (e.g. as strings of minute crystals in rhodochrosite–pyroxenoid fels or hematite–quartzite), the few spessartine porphyroblasts present have an overgrowth of yellow garnet. Spessartine is the sole mineral with Al in all the calderite-bearing samples studied, and layers bearing other Mn–Al-silicates like piemontite or ardennite do not contain calderitic garnet. This clearly points to Al availability as one of the controls on calderite formation and shows that, in the less Al-rich systems, Al was early sequestered into the spessartine garnet. As the spessartine porphyroblasts do not show early inclusions of calderitic garnet, nor an increase in Fe^{3+} content toward their rim, the inference is that calderitic garnet was not stable during spessartine growth but rather that the composition of the latter was buffered to very low Fe^{3+} values by the stable coexistence of hematite with pyroxenoid (cf. reaction [1]) – or even of hematite with rhodochrosite + quartz at a very early stage of the prograde history. It is difficult to assign the few chronological indications derived from textures [like rhodonite cores in pyroxmangite in Haute-Maurienne (Fig. 2 in *Chopin*, 1978) or the calderitic overgrowths on spessartine] to specific stages of the regional *P–T* evolution through eclogitic conditions. However, given the high-pressure stability of end-member calderite (*Lattard* and *Schreyer*, 1983) [and of pyroxmangite vs. rhodonite (*Maresch* and *Mottana*, 1976)], these overgrowths are tentatively assigned to the prograde history and, for the calderitic garnets, to late stages of the prograde history. With increasing pressure, pyroxmangite/rhodonite + hematite become unstable and, through the intergranular fluid, calderitic garnet may nucleate at some distance (within rhodochrosite pockets of the rhodochrosite–pyroxenoid

fels, or within the quartz groundmass of the quartzite) or grow on pre-existing spessartine crystals.

The textural relationships between colourless spessartine and the yellow spessartine overgrowth are most enlightening in this respect, considering that erosion of original features by late re-equilibration through volume diffusion is highly unlikely at such low temperatures as 500 °C. Figure 3d shows that 'intermediate garnet' (yellow spessartine) precipitates on a highly corroded and resorbed (colourless) spessartine core and that, therefore, the intergranular fluid attending such precipitation was clearly out of equilibrium with the spessartine core. An important implication is that the narrow gap (XFe = 0.10–0.15) between the core and overgrowth compositions does not reflect equilibrium (cf. Fig. 7) and cannot represent a miscibility gap, but rather the extent to which a calderite-(super)saturated intergranular fluid reacted with pre-existing garnet. Figure 3d suggests that this intermediate zone was corroded in turn as the outer calderite rim precipitated. However, this may not be the rule (cf. Fig. 3a, b) and calderite rims may also directly overgrow colourless spessartine, with or without corrosion (Figs. 2a, 3a).

Miscibility gaps in garnet?

According to textural and chemical evidence, and within analytical error, if a miscibility gap exists along the spessartine–calderite join, it has to be located within the chemical domain XFe = 0.40–0.65. However, immiscibility between two phases is difficult to prove. The only definitive petrological evidence would be exsolution of colourless spessartine within yellow garnet or vice versa, or, less obviously, of a yellow calderitic garnet within another yellow, more or less calderitic garnet. However, we did not find any evidence for exsolution.

There are few records of garnet immiscibility, and many of them are questionable. They basically rest on three types of evidence: i) garnet precipitates within a garnet matrix, which should be definitive evidence for exsolution; ii) a compositional gap between two coexisting but physically distinct garnet groups, iii) a compositional gap between growth zones of single garnet crystals, commonly oscillatory zoned.

Cressey (1978) reported HRTEM observations of unoriented precipitates of an iron-rich cubic phase in a grossular–almandine matrix, suggesting separation of two garnet phases in this system. However, the observation was convincingly reinterpreted by *Brearley* and *Champness* (1986) as magnetite precipitates in garnet.

Jamtveit (1991) recognized two compositional gaps in discrete coexisting garnet grains of the grandite series (Fig. 5b), one of which he interpreted as a possible miscibility gap on account of a similar gap found in other occurrences, compatible with unreversed experiments of *Huckenholz* and *Fehr* (1982), and suggested by the subregular solution model of *Engi* and *Wersin* (1987), based on these experiments. The coexistence of two Ti-rich garnets was reported by *Labotka* (1995) and taken as evidence for immiscibility between andraditic grossular and schorlomite. However, the very cuspate, corroded outline of the inclusion of a less Ti-rich garnet within a more Ti-rich garnet (his Fig. 1) can as well be reinterpreted as that of a relic, with growth of a second garnet generation and partial resorption of the early one. For a similar case of grossular-rich inclusions in pyropic garnet, *Wang* et al.

(2000) provided an elegant method to distinguish a stable immiscible pair from a disequilibrium coexistence in a single-phase field. If the pair results from immiscibility, decreasing temperature should lead to an enlargement of the compositional gap at the interface, whereas an initial compositional difference due to disequilibrium coexistence in a single-phase field will tend to homogenize upon annealing. However, such observation is practically limited to high-temperature garnets for diffusion to be effective and measurable; besides, it relies in its principle on the assumption that no uphill diffusion of Ca or Mg occurs for the envisaged complex compositions – a point that still needs to be ascertained.

The case of compositional gaps within oscillatory zoned crystals has received much attention in the grandite series (e.g. *Ivanova* et al., 1998 with references), including analysis at the very high spatial resolution required by oscillatory zoning down to nanometre-scale (*Pollok* et al., 2001). Molecular simulations (*Becker* and *Pollock*, 2002) suggest the existence of two miscibility gaps in the grandite series at XFe = 0.16–0.44 and XFe = 0.55–0.85, both with critical solvus temperatures of 370 K at XFe ≈ 0.25 and XFe ≈ 0.75. Such temperatures are too low to make miscibility gaps responsible for the compositional oscillations during near-equilibrium grandite growth (e.g. *Jamtveit*, 1991), rendering kinetic effects at the fluid–solid interface a more likely explanation for the fluctuations (*Becker* and *Pollock*, 2002). In any event, the spectacular intergrowth texture observed by *Yardley* et al. (1996) in a low-grade grossular-almandine overgrowth remains a unique and puzzling observation; it is the most suggestive of a miscibility gap, although the compositions involved are much more Fe-rich than expected from thermodynamic data.

Conclusion

The Mn garnets studied here reveal two compositional gaps that may be very reminiscent of those found by previous workers in the grandite system (even if a compilation of the latter data does not show much consistency, *Ivanova* et al., 1998) and of the immiscibility gaps derived from molecular modelling (*Becker* and *Pollock*, 2002). However, the textural evidence for heavy resorption of colourless spessartine kernels before the (over) growth of yellow garnet precludes an equilibrium process and, therefore, equilibrium compositions representative of a miscibility gap. The situation is less clear-cut for the calderite overgrowths on either colourless or yellow spessartine, but the weight of evidence also favours corrosion of the substrate, hence disequilibrium compositions. Therefore the compositional gap observed (XFe = 0.40–0.65) between these two yellow garnets represents only an upper bound to any miscibility gap in the spessartine–calderites series.

Acknowledgements

BCT thanks Ingo Braun (Bonn University) for access to the electron microprobe. Jacques Cassareuil is thanked for thin-section preparation, Michel Fialin for the help with the electron microprobe at Paris 6 University, the late Kurt Abraham, Bochum, for the first BSE pictures of calderite + spessartine, and Jean-Robert Kienast for introducing CC to the riches of Saint-Marcel, some time ago. This paper benefited from constructive reviews by Dominique Lattard and Simone Tumiati, and from corrections by Eric Essene, offered on very short notice.

References

Abs-Wurmbach I, Peters T, Langer K, Schreyer W (1983) Phase relations in the system Mn–Si–O: an experimental and petrological study. N Jb Mineral Abh 146: 258–279

Allen FM, Buseck PR (1988) XRD, FTIR, TEM studies of optically anisotropic grossular garnets. Am Mineral 73: 568–584

Amthauer G, Katz-Lehnert K, Lattard D, Okrusch M, Woermann E (1989) Crystal chemistry of natural Mn^{3+}-bearing calderite-andradite garnets from Otjosondu, SWA/Namibia. Zeit Krist 189: 43–56

Andrut M, Wildner M (2001) The crystal chemistry of birefringent natural uvarovites: Part I. Optical investigations and UV-VIS-IR absorption spectroscopy. Am Mineral 86: 1219–1230

Armbruster T, Birrer J, Libowitsky E, Beran A (1998) Crystal chemistry of Ti-bearing andratites. Eur J Mineral 10: 907–921

Becker U, Pollok K (2002) Molecular simulations of interfacial and thermodynamic mixing properties of grossular-andradite garnets. Phys Chem Minerals 29: 52–64

Bonazzi P, Menchetti S, Reinecke T (1996) Solid solution between piemontite and androsite-(La), a new mineral of the epidote group from Andros Island, Greece. Am Mineral 81: 735–742

Bondi M, Mottana A, Kurat G, Rossi G (1978) Cristallochimica del violano e della schefferite di St. Marcel (Valle d'Aosta). Rend SocItal Mineral Petrol 34: 15–25

Brearley AJ, Champness PE (1986) Magnetite exsolution in almandine garnet. Mineral Mag 50: 621–633

Brown P, Essene EJ, Peacor DR (1978) The mineralogy and petrology of manganese-rich rocks from St. Marcel, Piemont, Italy. Contrib Mineral Petrol 67: 227–232

Brugger J, Gieré R, Graeser S, Meisser N (1997) The crystal chemistry of roméite. Contrib Mineral Petrol 127: 136–146

Bühn B, Okrusch M, Woermann E, Lehnert K, Hoernes S (1995) Metamorphic evolution of Neoproterozoic manganese formations and their country rocks at Otjosondu, Namibia. J Petrol 36: 463–496

Cenki-Tok B, Ragu A, Armbruster T, Chopin C, Medenbach O (2006) Mn- and rare-earth-rich epidote-group minerals in metacherts: androsite-(Ce) and vanadoandrosite-(Ce). Eur J Mineral, under review

Chakhmouradian AR, McCammon CA (2005) Schorlomite: a discussion of the crystal chemistry, formula, and inter-species boundaries. Phys Chem Minerals 32: 277–289

Chopin C (1978) Les paragenèses réduites ou oxydées de concentrations manganésifères des ⟨⟨schistes lustrés⟩⟩ de Haute-Maurienne (Alpes françaises). Bull Minéral 101: 514–531

Chopin C (1981a) Talc-phengite: a widespread assemblage in high-grade pelitic blueschists of the Western Alps. J Petrol 22: 628–650

Chopin C (1981b) Mise en évidence d'une discontinuité du métamorphisme alpin entre le massif du Grand Paradis et sa couverture allochtone (Alpes occidentales françaises). Bull Soc géol France 23: 297–301

Cressey G (1978) Exsolution in almandine-pyrope-grossular garnet. Nature 271: 533–534

Dal Piaz GV, Di Battistini G, Kienast J-R, Venturelli G (1979) Manganiferous quartzitic schists of the Piemonte ophiolitic nappe. Mem Sc Geol Padova 32: 1–24

Dal Piaz GV, Cortiana G, Del Moro A, Martin S, Pennacchioni G, Tartarotti P (2001) Tertiary age and paleostructural inferences of the eclogitic imprint in the Austroalpine outliers and Zermatt-Saas ophiolite, western Alps. Int J Earth Sci 90: 668–684

Damour A (1841) Sur la roméite, nouvelle espèce minérale, de St Marcel, Piémont. Annales des Mines, 3rd series, 20: 247

Dasgupta S, Bhattacharya PK, Banerjee H, Fukuoka M, Majumdar N, Suprya R (1987) Calderite-rich garnets from metamorphosed manganese silicate rocks of the Sausar group, India, and their derivation. Mineral Mag 51: 577–583

Dunn PJ (1979) On the validity of calderite. Can Mineral 17: 569–571

Enami M, Cong B, Yoshida T, Kawabe I (1995) A mechanism for Na incorporation in garnet – an example from garnet in orthogneiss from the Su–Lu terrane, eastern China. Am Mineral 80: 475–482

Engi M, Wersin P (1987) Derivation and application of a solution model for calcic garnets. Schweiz mineral petrogr Mitt 67: 53–73

Fudral S, Deville E, Pognante U, and 11 authors (1994) Carte géol. France (1/50 000), feuille Lanslebourg–Mont-d'Ambin (776). Orléans: BRGM

Gramaccioli CM, Griffin WL, Mottana A (1980) Tiragalloite, $Mn_4[AsSi_3O_{12}(OH)]$, a new mineral and the first example of arsenatotrisilicate. Am Mineral 65: 947–952

Gruppo Ofioliti (1977) Escursione ad alcuni giacimenti a Cu–Fe e Mn della falda piemontese, Alpi occidentali: 10–13 ottobre 1977. Ofioliti 2: 241–263

Hârtopanu P, Vanghelie I, Stelea G, Calinescu E (1997) On the presence of garnet-spessartine-calderite in the Delinesti Mn–Fe deposit. Romanian J Mineral 78: 45–52

Huckenholz HG, Fehr KT (1982) Stability relationships of grossular + quartz + wollastonite + anorthite. II. The effect of grandite-hydrograndite solid solution. N Jb Mineral Abh 145: 1–33

Ivanova TI, Shtukenberg AG, Punin Yu O, Frank-Kamenetskaya OV, Sokolov PB (1998) On the complex zonality in grandite garnets and implications. Mineral Mag 62: 857–868

Jamtveit B (1991) Oscillatory patterns in hydrothermal grossular-andratite garnet: nonlinear dynamics in regions of immiscibility. Am Mineral 76: 1319–1327

Jamtveit B, Ragnarsdottir KV, Wood BJ (1995) On the origin of zoned grossular-andradite garnets in hydrothermal systems. Eur J Mineral 7: 1399–1410

Kenngott A (1853) Das Mohs'sche Mineralsystem (Piemontit), p 75

Klein C (1966) Mineralogy and petrology of the metamorphosed Wabush iron formation, southwestern Labrador. J Petrol 7: 246–305

Labotka TC (1995) Evidence for immiscibility in Ti-rich garnet in a calc-silicate hornfels from northeastern Minnesota. Am Mineral 80: 1026–1030

Lattard D, Schreyer W (1983) Synthesis and stability of the garnet calderite in the system Fe–Mn–Si–O. Contrib Mineral Petrol 84: 199–214

Maresch WV, Mottana A (1976) The pyroxmangite-rhodonite transformation for the $MnSiO_3$ composition. Contrib Mineral Petrol 55: 69–79

Martin S, Kiénast J-R (1987) The HP-LT manganiferous quartzites of Praborna, Piemonte ophiolite nappe, Italian Western Alps. Schweiz Mineral Petrogr Mitt 67: 339–360

Martin S, Lombardo B (1995) Sursassite, spessartine, piemontite in Fe–Mn metacherts from Lago Bleu, upper Val Varaita (western Alps). Boll Mus reg Sci Nat Torino 13 [Suppl 2]: 103–130

Martin S, Polino R (1984) Le metaradiolariti a ferro di Cesana (Valle Di Susa-Alpi Occidentali). Mem Soc Geol It 29: 107–125

Martin S, Tartarotti P (1989) Polyphase HP metamorphism in the ophiolitic glaucophanites of the lower St. Marcel Valley (Aosta, Italy). Ofioliti 14: 135–156

Meisser N, Perseil EA, Brugger J, Chiappero PJ (1999) Strontiomelane, $SrMn^{4+}{}_6Mn^{3+}{}_2O_{16}$, a new mineral species of the cryptomelane group from St Marcel-Praborna, Aosta Valley, Italy. Can Mineral 37: 673–678

Mottana A, Rossi G, Kracher A, Kurat G (1979) Violan revisited: Mn-bearing omphacite and diopside. TMPM Tschermaks Min Petr Mitt 26: 187–201

Muir Wood R (1982) The Laytonville Quarry (Mendocino County, California) exotic bloc: iron-rich blueschist-facies subduction-zone metamorphism. Mineral Mag 45: 87–99

Mukhopadhyay S, Roy S, Fukuoka M, Dasgupta S (2002) Controls of evolution of mineral assemblages in ultrahigh-temperature metamorphosed Mn-carbonate-silicate rocks from the Eastern Ghats Belt, India. Eur J Mineral 14: 73–83

Pasero M, Reinecke T (1991) Crystal chemistry, HRTEM analysis and polytypic behaviour of ardennite. Eur J Mineral 3: 819–830

Pasero M, Reinecke T, Fransolet A-M (1994) Crystal structure refinements and compositional control of Mn–Mg–Ca ardennites from the Belgian Ardennes, Greece, and the Western Alps. N Jb Mineral Abh 166: 137–167

Pollok K, Jamtveit B, Putnis A (2001) Analytical transmission electron microscopy of oscillatory zoned grandite garnets. Contrib Mineral Petrol 141: 358–366

Reinecke T (1987) Manganoan deerite and calderitic garnet from high-pressure metamorphic Fe–Mn-rich quartzites on Andros Island, Greece. Mineral Mag 51: 247–251

Reinecke T (1991) Very-high-pressure metamorphism and uplift of coesite-bearing sediments from the Zermatt-Saas zone, Western Alps. Eur J Mineral 3: 7–17

Rolland Y, Lardeaux JM, Guillot S, Nicollet C (2000) Syn-convergence extension, vertical pinching and contrasted metamorphic units on the western edge of the Gran Paradise massif (French–Italian Alps). Geodinamica Acta 13: 133–148

Sastri GGK (1963) Note on a chrome and two manganese garnets from India. Mineral Mag 33: 508–511

Schreyer W, Abraham K (1977) Howieite and other high-pressure indicators from the contact aureole of the Brezovica, Yugoslavia, peridotite. N Jb Miner Abh 130: 114–133

Stalder M, Rozendaal A (2005) Calderite-rich garnet and franklinite-rich spinel in amphibolite-facies hydrothermal sediments, Gamsberg Zn–Pb deposit, Namaqua Province, South Africa. Can Mineral 43: 585–599

Vermaas FHS (1952) Manganese-iron garnet from Otjosondu, South-West Africa. Mineral Mag 29: 946–951

Wang L, Essene EJ, Zhang Y (2000) Direct observation of immiscibility in pyrope-almandine-grossular garnet. Am Mineral 85: 41–46

Yardley BWD, Condliffe E, Lloyd GE, Harris DHM (1996) Polyphase garnets from west Ireland: two-phase intergrowths in the grossular-almandine series. Eur J Mineral 8: 383–392

Author's address: *C. Chopin* (corresponding author; e-mail: chopin@geologie.ens.fr), Laboratoire de Géologie, UMR 8538 du CNRS, Ecole normale supérieure, 24 rue Lhomond, 75005 Paris, France